Seismic Vulnerability Assessment of a Set of Concrete Gravity Dams

Saeid Ghasemi Gavabar[1], Mohammad Alembagheri[2], Behrang Esmi[1]

1- M.Sc., School of Civil Engineering, University of Tehran, Tehran, Iran
2- Assistant Professor, Department of Civil and Environmental Engineering, Tarbiat Modares University, Tehran, Iran

Email: ghasemisaeid@ut.ac.ir

Abstract

Since dams are very important structures, vulnerability assessment and evaluation of their safety against destructive phenomena are significant. Vulnerability assessment and prediction of dam's damage due to earthquake with a variety of intensities can provide helpful information that would be very useful and effective in the proper management of probable crises. One of the useful tools in assessing earthquake damage in concrete dams is the production of their related fragility curves. Due to the vulnerability of concrete dams to tensile cracking, a new concept of damage index (DI) according to tensile cracking has been developed. Also because of dependency of fragility curve to limit states of engineering demand parameters (EDP), limit states have been defined according to tensile cracking in dams. Studies on the production of fragility curves on concrete gravity dams are very limited and mostly not comprehensive in a way fragility curve are normally produced only for one type of dams or with one height and one figuration. In this paper, fragility curves have been plotted for a set of concrete gravity dams, such as Pine Flat, Koyna and Shafarood. Through extensive studies on different sample dams' structural performances comparisons are made possible using fragility curve.

Keywords: concrete gravity dams, damage index, nonlinearity, fragility curve, seismic vulnerability.

1. INTRODUCTION

About 10% of high dams in the world are concrete gravity dams [1]. They impound large reservoirs of water and play a key role in water management, flood prevention and power generation. The consequences of failure of a high concrete dam could be very catastrophic. Hence, assuring their proper performance specifically during extreme events like earthquakes is of great importance. Yet, many dams are aging and most were designed at a time with limited seismic field data. Most of the existing dams have been in service for several years and the effect of age has made them too vulnerable to endure severe natural hazards like earthquake. Therefore, seismic vulnerability assessment of concrete gravity dams is very important now. Due to new design guidelines for severe earthquake conditions and dams, most of the existing dams fail to provide the safety criteria of new design guideline [2].

Damage index (DI) measures the amount of damage and degradation rate that is inflicted to a structure. The idea of describing the damage states of the structure with one number is marvelous because of its plainness [3]. DIs are obtained with empirical and theoretical approaches. In the case of concrete gravity dams, because there is a limited data base of field and experimental observation of damages, the numerical methods for estimation of DI are preferred. One well-known method for computing the structural capacities is the incremental dynamic analysis (IDA) [4]. In an IDA, the intensity of ground motion applied to the base of the structure is incrementally increased until the structure collapses [5].

Damage indexes are usually normalized so that they have zero value when the structure is in no-damage state and unit value when failure or total collapse of the structure occurs. The damage state of the structure can be defined in several ways: a binary damage state (failure/no failure) and a discrete valued damage state by using qualitative indicators such as none, minor, reparable, severe and failure [4]. In concrete gravity dams due to lack of empirical data, determining such qualitative indicators of damage for gravity dams is not easily possible.

The DIs are divided into two general categories: local and global DIs. A local DI is an indicator of damage for a part of a structure, whereas a global DI gives an estimate of overall damage imposed on the structure. In addition, the DIs are separated into cumulative and non-cumulative ones. Those indexes that can consider the accumulation effect of seismic excitation to structural damages are called cumulative indexes [4].

Concrete gravity dams can be divided into three major zones on the basis of crack propagation; (i) base/dam-foundation interface region, (ii) main body of dam, and (iii) around neck region. Among all these three regions (i) and (iii) are most likely to have cracks; however, in some rare cases under extreme events, region (ii) can also undergo cracks [2]. Therefore, in this paper a damage index has been proposed to monitor tensile damage (d_t) in concrete gravity dams.

Fragility curves describe the probability of damage in a structure at various levels of earthquake. It is the best way to estimate and evaluate the vulnerability of potential damage in future earthquakes. Fragility curves can also be used for prioritizing retrofitting, pre-earthquake planning, and loss estimation tools. The development of fragility or vulnerability assessment function is generally based on expert opinion, analytical methods, and the damage data of structures from past events [6].

The past vulnerability data are very scarce in case of concrete dams. Therefore, analytical methods have been used to obtain fragility curves. There are two approaches used for the development of analytical fragility curves (a) based on demand of structures [9, 10] and (b) based on damage indexes [11, 12]. The first approach is suitable for design purposes [13] while the second methodology is appropriate for the damage evaluation due to its ability to define damage states [24]. In the present paper, incremental dynamic analysis (IDA) method is used for the categorization of the limit states on engineering demand parameters and development of fragility curve by considering 30 earthquake ground motions [2]. Two local and one global damage indexes have been developed according to tensile damage in base and around the neck of the dams.

This study is an attempt to determine the limit states and define a new local and global damage index (DI) for a set of concrete gravity dams and plot their related fragility curves according to their limit states. Using Pine Flat, Koyna and Shafarood dams as case study, their numerically modeled along with its full reservoir utilizing finite element method in three analysis cases (Pine Flat, Koyna and Shafarood) to assess the performance of the dam's structure in intact situations. Only material nonlinearity is considered in modeling. The dam-reservoir system is modeled based on Eulerian-Lagrangian approach. Thirty proper ground motion records are selected for the purpose of analysis. Several EDPs for each case are calculated in terms of IMs. Limit states are defied in every level of $S_a(T_1)$ according to progress of tensile damage in base or neck of the dams. Finally, the seismic fragility curves of every EDP and EDPs for a set of concrete gravity dams are generated.

2. INCREMENTAL DYNAMIC ANALYSIS

Incremental dynamic analysis is a parametric analysis that estimates more thoroughly structural performance under seismic loads. It involves subjecting a structural model to some ground motion records, each scaled to multiple levels of intensity, thus producing some curves of response parameterized versus intensity level [18]. As mentioned earlier, the IDA approach involves performing nonlinear dynamic analyses to a structure under a suite of ground motion records; each of the selected records is scaled to several intensity levels. Herein, the spectral acceleration at the natural period of the concrete gravity dam structure (S_a (T_n)) is selected as an intensity measure (IM) used to describe ground motion characteristics. The first reason behind this selection is that seismic demand estimates are strongly correlated with the linear-elastic spectral acceleration at natural period of the structure (T_n). Moreover, based on 4 criteria (i.e. practicality, sufficiency, effectiveness and efficiency) Hariri et al. showed that S_a (T_n) is an optimal IM for seismic performance assessment of concrete gravity dam structures [7]. Each of the records has been scaled to multiple levels of Sa (T_1,5%) from zero to 1 g that have been arranged in 0.1 g steps. A set of incremental time history analyses was performed by applying scaled ground motions and desired EDP values were monitored during each analysis.

3. GRAVITY DAM-RESERVOIR NONLINEAR NUMERICAL MODELS

The tallest non-overflow monolith of concrete gravity dams is chosen along with its full reservoir, as shown in Figure 1. The two-dimensional dam-reservoir system is numerically analyzed using the finite element method based on Eulerian formulation (pressure-based elements) for the reservoir, and Lagrangian formulation (displacement-based elements) for the dam body in plane-stress manner. The foundation is assumed rigid. The reservoir length is considered to be five times the dam height and transmitting boundary condition is assigned to its truncated far-end. A pressure-free condition is assumed for the free surface of the reservoir. The finite element equations of the dam body are coupled with the finite element equations of the reservoir through a coupling matrix which relates the hydrodynamic pressure of the reservoir to the equivalent forces on the dam structure. For a detailed description of these models, one can refer to [19]. The selected earthquakes are uniformly applied to the rigid foundation beneath the dam body.

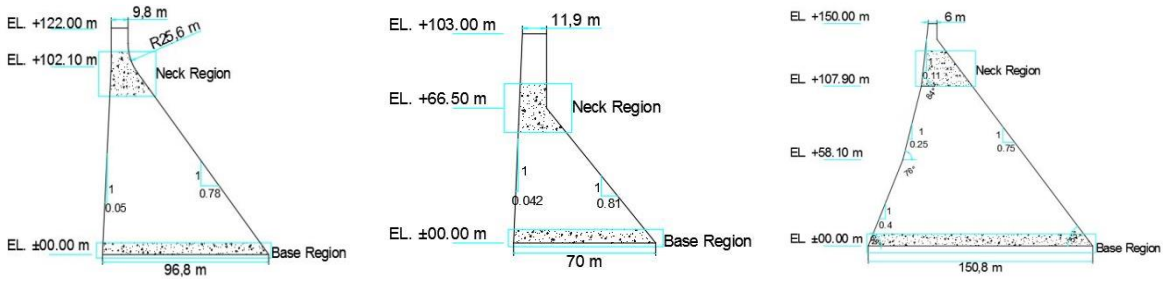

Pine Flat Koyna Shafarood

Figure 1. (a) Tallest non-over-flow monolith of Pine Flat dam, Koyna dam and Shafarood dam

Only material nonlinearity is taken into account. The material nonlinearity of mass concrete is modeled using plastic-damage method which is a continuum homogeneous damage mechanics approach. Considering only the tensile damage as the main material failure for the gravity dam, the stiffness degradation of mass concrete in tension, beyond the tensile strength (f_t) is modeled as:

$$E = (1-d_t)E_0 \tag{1}$$

where E_0 is the initial (undamaged) modulus of the material, and d_t is the tensile damage parameter which is assumed to be a function of the plastic strains. The tensile damage parameter can take values from zero, representing the undamaged material, to one, which represents total loss of strength [20]. For a detailed description of the model, one can consult [21]. The considered constitutive behavior of mass concrete in this study is shown in Figure 2. The curve and parameters have been selected based on the experimental data [22]. The material properties for all three models are tabulated in Table 1. They are assumed the same for both static and dynamic analyses.

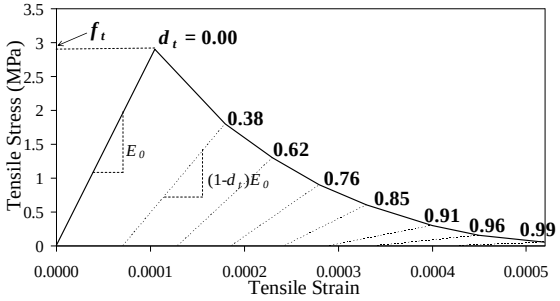

Figure 2. Constitutive behavior of mass concrete in uniaxial tension

Table 1. Material properties used in this study

Material	Property	Value
Concrete	Mass density (kg/m^3)	2400
	Undamaged Young's modulus (GPa)	27.58
	Poisson's ratio	0.2
	Tensile strength (MPa)	2.9
Water	Mass density (kg/m^3)	1000
	Bulk modulus (GPa)	2.07

3.1. LOCAL AND GLOBAL DAMAGE INDEX

During seismic events, the dam body may separately crack from its base or neck. Hence, based on the plastic-damage model for cracking response of the concrete, two damage-based indices can be locally defined on the cracking-susceptible sub-regions of the dam body. These sub-regions were depicted in Figure 3 as base and neck regions. The local damage indices, *DI*, for both regions can be defined as:

$$DI_i = \frac{\sum_{e|i} d_{t|e} A_e}{\sum_{e|i} A_e} \qquad i = base\ or\ neck \tag{2}$$

where $d_{t|e}$ is the tensile damage of element e with area of A_e. The summation is done on the entire region i. It simply calculates the weighted average of the damage variables over the prescribed base or neck regions. Therefore, it is a measure of the amount of damage that the dam may locally experience. $DI_i = 0$ means that no element cracks. $DI_{base} = 1$ shows that the crack has penetrated through the entire dam base, and $DI_{neck} = 1$ shows total complete damage of the dam neck, however, this diffused cracking is not a realistic cracking pattern for mass concrete structures like gravity dams. If damage index had been provided for the entire dams, it would present global damage index. The energy-based EDPs include the energy dissipated through cracking damage process, *ED*, which can also be considered as a global measure of damage imposed to the dam body.

3.2. REPRESENTATIVE EDPS

The EDPs are the outcome of the nonlinear finite element analysis of the models that classify the dams seismic demand. The adopted EDPs for each case are described in Table 2. They are categorized in three groups: (1) deformation-based, (2) damage-based, (3) energy-based. The deformation-based EDPs are crest maximum relative displacement. Because the dam body has un-symmetric geometry, the crest relative displacements can be separately monitored into the upstream (US) or the downstream (DS) directions.

Table 2. The adopted EDPs for all analyses model

Category	EDP	Explanation
Deformation-based	D_{us}	Crest maximum relative displacement in the US direction
	D_{ds}	Crest maximum relative displacement in the DS direction
	D_{max}	Crest maximum absolute relative displacement
Damage-based	DI_i, i = base or neck	Local damage index
	DI_{Total}	Global damage index
Energy-based	*ED*	Energy dissipated through cracking damage

4. NAMING OF CREATED DAMAGE PATTERNS

According to propagation of tensile damage imposed on concrete gravity dams in different intensities of ground motion, three limit states have been defined.

a: This letter represents the initiation of the tensile damage (cracking) at the first element in the base of the dams. Within this time dams have completely a linear behavior named immediate occupancy (IO).

b: This letter represents the initiation of tensile damage (cracking) at the first element in the neck area of the dams. In all of the models this type of damage occurs after initiation and propagation tensile damage in the base of the dam named medium damage (MD).

c: this letter defines a throughout cracking line that has occurred along the neck area. Due to sliding the monolith that is located above cracking line, this situation is very critical for the dam and downstream of the dam. Therefore, this type of damage has been named high damage (HD).

5. LIMIT STATES ACCORDING TO DRIFT

In table 3 the comparison of the dam's drift according to different intensities have been demonstrated. All the numbers in table 3 are presented in percent (%). As shown here, the initiation of tensile cracking has occurred in $Drift_{us}$, 0.014%, 0.01% and 0.007% and in $Drift_{max,}$ 0.016%, 0.031% and 0.018% for Pine Flat, Koyna and Shafarood respectively. Also, the initiation of tensile cracking around the neck has been in $Drift_{us,}$ 0.023%, 0.012% and 0.016% and in $Drift_{us,}$ 0.036%, 0.057% and 0.030% respectively for the mentioned dams. Finally, the ultimate value for $Drift_{us}$ are 0.026%, 0.015% and 0.019% and for $Drift_{max}$ are 0.053%, 0.070% and 0.35% respectively for Pine Flat, Koyna and Shafarood dam.

Table 3. Comparison of dam's drift

	$Drift_{us}$%			$Drift_{ds}$%			$Drift_{max}$%		
$S_a(T_1)$	PineFlat	Koyna	Shafarood	PineFlat	Koyna	Shafarood	PineFlat	Koyna	Shafarood
0.1g	-0.007	-0.008	-0.003	0.009	0.022	0.010	0.009	0.022	0.010
0.2g	-0.014	-0.010	-0.005	0.016	0.031	0.014	0.016	0.031	0.014
0.3g	-0.019	-0.011	-0.007	0.025	0.042	0.018	0.025	0.042	0.018
0.4g	-0.023	-0.012	-0.010	0.036	0.056	0.022	0.036	0.057	0.022
0.5g	-0.026	-0.015	-0.013	0.053	0.070	0.026	0.053	0.070	0.026
0.6g	-0.029	-0.016	-0.016	0.078	0.094	0.030	0.078	0.094	0.030
0.7g	-0.032	-0.020	-0.019	0.099	0.108	0.034	0.099	0.108	0.035
0.8g	-0.034	-0.022	-0.023	0.129	0.181	0.039	0.129	0.181	0.040
0.9g	-0.036	-0.023	-0.027	0.163	0.242	0.045	0.164	0.242	0.047
1g	-0.030	-0.027	-0.036	0.239	0.319	0.050	0.239	0.319	0.054

6. FRAGILITY CURVE DEVELOPMENT

In this study, the probability of exceeding a damage state given a level of ground motion (i.e. seismic fragility) is calculated for three previously defined limit states.

Having previously defined bounds of three damage states and seismic demand values (resulted from IDA), seismic fragility of the damage state D_i is the conditional probability that a concrete dam has a state of damage exceeding the damage state D_i at a specific S_a level, which is shown in closed form as Eq. (3).

$$\left[D > d \mid S_a\right] = P\left[X > x_i \mid S_a\right] = 1 - \phi\left[\frac{\ln(x_i - \alpha)}{\beta}\right] \tag{3}$$

$$\alpha = \ln\mu - \frac{1}{2}\beta^2 \tag{4}$$

$$\beta = \sqrt{\ln\left[1 + \left(\frac{\sigma}{\mu}\right)^2\right]} \tag{5}$$

Where $\phi(.)$, is the standard normal cumulative distribution function and X_i is the upper bound for each damage state as presented in section 5.

The parameters α and β as defined in Eqs. 4 and 5 depend on the S_a level. σ and μ are respectively the mean and standard deviation of seismic demand values in each S_a level.

6.1. FRAGILITY CURVE DEVELOPMENT FOR A SET OF CONCRETE GRAVITY DAM

The purpose of this study is to provide fragility curves for a set of concrete gravity dams whose heights are between 100 m to 150 m.

All of the limit states for the plotting of the figure 3 are the average of the three dams limit states. And also, the standard normal cumulative distribution function parameters have been obtained with the averaging of three models. Table 4 represents three limit states for a set of concrete gravity dams as (IO, MD and HD).

Table 4. Limit states for concrete gravity dams with the height between 100-150 m

	D_{us}(cm)	D_{ds}(cm)	D_{max}(cm)	DI_{base}	DI_{neck}	DI_{Total}	E_D(j)
IO	-1.22	2.62	2.62	0.1283	0	0.00062	6525
MD	-2.14	4.86	4.86	0.2884	0.0177	0.0191	29042.7
HD	-2.54	6.27	6.31	0.3352	0.0334	0.0272	44651.38

As seen in figure 3, the Pine Flat and Koyna EDPs fragility curves moved forward but Shafarood EDPs fragility curves were transferred to the rear side. Finally, the concrete gravity dams' probability of exceedance with hight ranging between 100 to 150 meters are summarized in the following.

The D_{us} (figure 3 (a)) probability of exceedance for three average limit states are 99%, 72% and 55% respectively according to S_a=0.6g. Also, the D_{ds} and D_{max} (figure 3 (b, c)) probability of exceedance for three average limit states are 100%, 88% and 56% respectively based on S_a=0.6g. DI-base fragility curves have been demonstrated in figure 3 (*d*) whose the probability of exceedance for three limit states are 100%, 89% and 61% respectively based on S_a=0.6g. figure 3 (*e*) represented the DI_neck fragility curves whose the probability of exceedance for two limit states are 74% and 50% respectively according to Sa=0.6g. The DI_Total (figure 3 (f)) probability of exceedance for three limit states are 100%, 73% and 55% respectively according to S_a=0.6g. And finally ED fragility curves are demonstrated in figure 3 (g) whose the probability of exceedance for three limit states are 100%, 80% and 54% respectively based on S_a=0.6g.

7. CONCLUSIONS

In this paper, the seismic behavior of a set of concrete gravity dams has been studied through nonlinear dynamic analyses. The dams were modeled along with their reservoirs utilizing the finite element method. The material nonlinearity was considered in all models. Thirty far-field ground motion records were selected for the purpose of analysis. Concrete dams were subjected to selected earthquakes which scaled according to spectral acceleration from 0.1g to 1g. Seven EDPs have been defined in the finite element model. Two local and one global damage indexes have been introduced according to tensile damage (d_t) and element areas. Three limit states have been defined according to propagation of tensile cracking in the base and around the neck of the dams. That Shafarood behavior is nearly linear compared with two other dams due to the former's shape and large width. According to the defined limit states for EDPs, the seismic fragility curve that estimates the conditional exceeding probability of damage at a given ground motion intensity has been plotted for all EDPs in three models whose Shafarood EDPs probability of exceedance are less than the two others' same EDPs probability of exceedance. Finally, because of having a collectivity of fragility curves for concrete gravity dams with 100-150 meters height, fragility curves have been developed for seven EDPs according to spectral acceleration which can be useful for vulnerability assessment of existing concrete gravity dams which experience a lot of earthquakes.

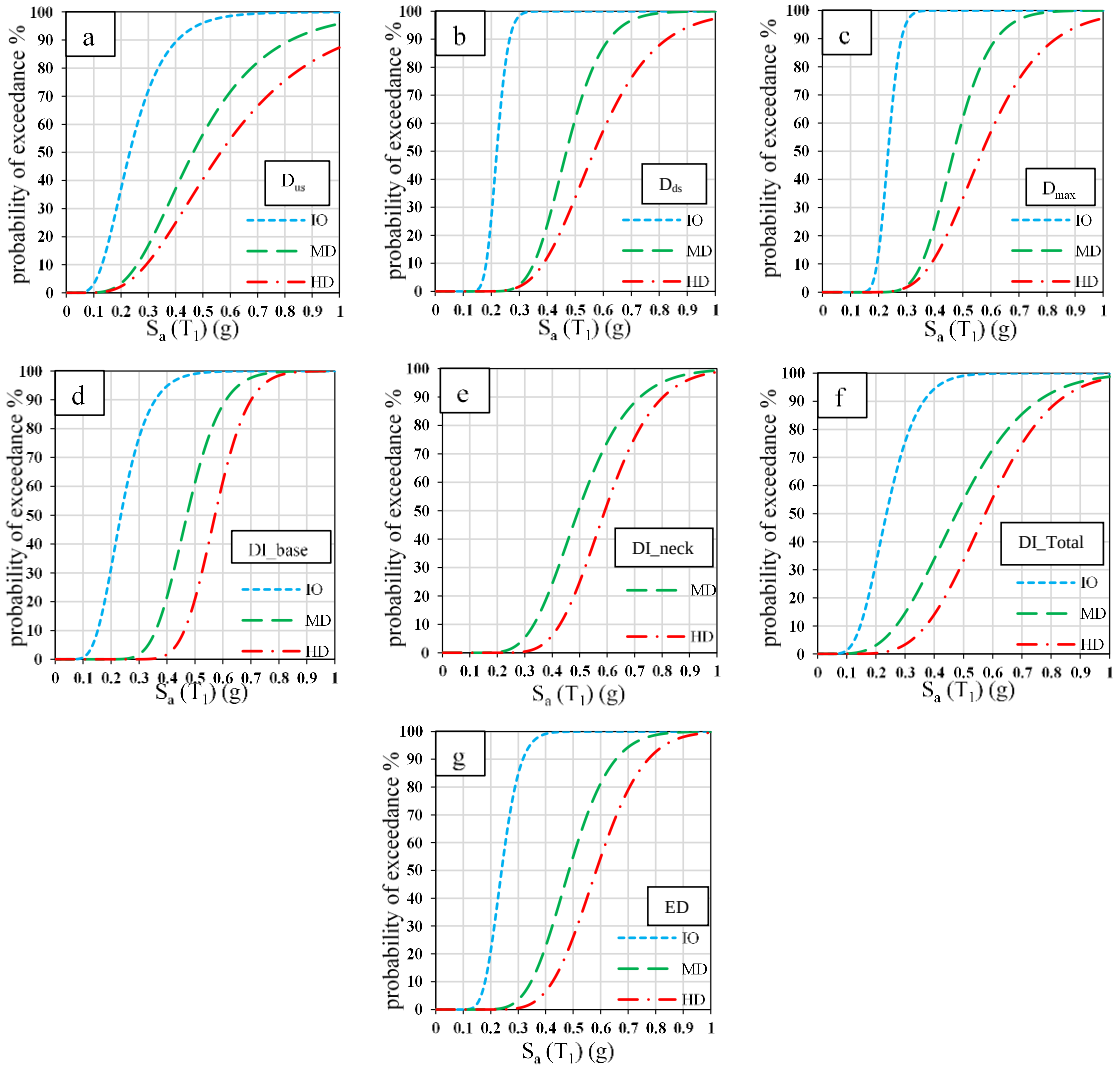

Figure 3. Fragility curves for a set of concrete gravity dams EDPs according to three limit states

8. REFERENCES

1. International Commission on Large Dams (2016) Selecting seismic parameters for large dams - Guidelines, ICOLD Bulletin 148.
2. Ansari MI, Agarwal P. Categorization of damage index of concrete gravity dam for the health monitoring after earthquake. Journal of Earthquake Engineering. 2016 Nov 16;20(8):1222-38.
3. Ghobarah A, Abou-Elfath H, Biddah A. Response-based damage assessment of structures. Earthquake engineering & structural dynamics. 1999 Jan 1;28(1):79-104.
4. Alembagheri M, Ghaemian M. Seismic assessment of concrete gravity dams using capacity estimation and damage indexes. Earthquake Engineering & Structural Dynamics. 2013 Jan 1;42(1):123-44.
5. Vamvatsikos D, Cornell CA. Incremental dynamic analysis. Earthquake Engineering & Structural Dynamics. 2002 Mar 1;31(3):491-514.
6. Porter KA, Kiremidjian AS. Assembly-based vulnerability of buildings and its uses in seismic performance evaluation and risk-management decision-making. SPA Risk LLC; 2000.
7. Hariri MA, Saouma VE (2016) Probabilistic seismic demand model and optimal intensity measure for concrete dams. Structural Safety 59:67-85
8. Ghanaat Y (2004) Failure modes approach to safety evaluation of dams. In: Proceedings of 13th World Conference on Earthquake Engineering, Vancouver, B.C., Canada.
9. Shinozuka M, Feng MQ, Lee J, Naganuma T. Statistical analysis of fragility curves. Journal of engineering mechanics. 2000 Dec;126(12):1224-31.
10. Dimova SL, Hirata K. Simplified seismic fragility analysis of structures with two types of friction devices. Earthquake engineering & structural dynamics. 2000 Aug 1;29(8):1153-75.
11. Smyth AW, Deodatis G, Franco G, He Y, Gurvich T. Evaluating earthquake retrofitting measures for schools: a cost-benefit analysis. School Safety and Security: Keeping Schools Safe in Earthquakes. 2004 Aug 4:208-16.
12. Karim KR, Yamazaki F. A simplified method of constructing fragility curves for highway bridges. Earthquake engineering & structural dynamics. 2003 Aug 1;32(10):1603-26.
13. Bazzurro P, Cornell CA, Menun C, Luco N, Motahari M. Advanced Seismic assessment guidelines. Report for Pacific Gas and Electric-PEER Lifelines Program, Task, pp: 507.
14. Lupoi A, Callari C. The role of probabilistic methods in evaluating the seismic risk of concrete dams. InProtection of Built Environment Against Earthquakes 2011 (pp. 309-329). Springer Netherlands.
15. FEMA (2003) NEHRP recommended provisions for seismic regulations for new buildings and other structures (FEMA 450). National Earthquake Hazards Reduction Program, Part 1: PROVISIONS. Prepared by the Building Seismic Safety Council for the Federal Emergency Management Agency, Washington, DC, USA.
16. PEER (Pacific Earthquake Engineering Research Center). (2014). "Ground motion database." CA.
17. Hariri-Ardebili MA, Saouma VE. Collapse Fragility Curves for Concrete Dams: Comprehensive Study. Journal of Structural Engineering. 2016 Apr 28;142(10):04016075.
18. Vamvatsikos D, Cornell CA. Incremental dynamic analysis. Earthquake Engineering & Structural Dynamics. 2002 Mar 1;31(3):491-514.
19. Heidary-Torkamani H, Bargi K, Amirabadi R, McCllough NJ. Fragility estimation and sensitivity analysis of an idealized pile-supported wharf with batter piles. Soil Dynamics and Earthquake Engineering. 2014 Jul 31; 61:92-106.
20. Calayir Y, Dumanoğlu AA, Bayraktar A (1996) Earthquake analysis of gravity dam-reservoir systems using the Eulerian and Lagrangian approaches. Computers & Structures 59:877-890
21. Alembagheri M, Ghaemian M (2016) Seismic performance evaluation of a jointed arch dam. Structure and Infrastructure Engineering 12:256-274
22. Lee J, Fenves GL (1998) A plastic-damage concrete model for earthquake analysis of dams. Earthquake Engineering and Structural Dynamics 27:937-956